The role of viscous deformation in the machining of polymers

K.Q. Xiao, L.C. Zhang*

School of Aerospace, Mechanical and Mechatronic Engineering, The University of Sydney, Sydney, NSW 2006, Australia

Abstract

This study aims to evaluate the machinability of typical thermoplastic and thermosetting polymers and understand the effect of their viscous properties on surface integrity, chip formation and machining forces. The interaction between the strain rate and temperature during machining was particularly addressed. It was found that the viscous deformation of a polymer plays a decisive role in determining the quality of a machined surface. To minimize the surface roughness, for instance, the machining conditions must be selected in such a way that the material removal deformation falls in the regime without visco-plastic scaling/tearing and brittle cracking. The optimal machining condition must be based on the polymer properties, such as the glass transition temperature, fracture toughness and molecular mobility. The shear stress in the shear plane of chipping is a good measure of the coupled effect of strain rate and temperature rise. In addition, the study discovered two new types of chips whose deformation and curling were in close relation to the surface integrity of the machined components.
© 2002 Elsevier Science Ltd. All rights reserved.

Keywords: Polymer machinability; Surface finishing; Material property

1. Introduction

Machining of polymeric materials has been increasingly used and has become necessary when the quantity of precious items does not justify the cost of tooling for moulds or extrusion dies, or when a product needs a costly dimensional accuracy, such as polymer lenses.

Similar to the machining of metals, factors that influence the quality of a machined component can be divided into three categories. The first includes machine and environmental variables such as slide straightness, temperature stability and vibration isolation, which control the large-scale dimensions. Their effects on the machining of metals have been widely studied in detail [1–4], although there is

---

* Corresponding author. Tel.: +61-2-9351-2835; fax: 61-2-9351-3760.
  E-mail address: zhang@mech.eng.usyd.edu.au (L.C. Zhang).

little work on polymers. The second group is associated with the tool design and machining conditions such as rake angle, tip radius, depth of cut and cutting speed. The influence of these factors on surface roughness, chip formation, tool wear, gumming and burning of polymeric materials has been investigated by several researchers [5–11]. It was concluded that rake angle [5,9] and transverse feed [11] are important parameters that determine the surface roughness in polymer machining. In addition to the processing variables above, the effect of physical and chemical properties of polymeric materials is much more pronounced in machining. Because of their visco-elastic behavior, it is difficult to uncover the relationship between machinability and material properties.

Some early studies on polymer machining [5,9,12–14] tried to investigate the relationship of the material parameters, such as glass transition temperature, melting temperature, viscosity and relaxation, with the surface finish of workpieces. For example, Smith [13] considered the effect of the glass transition temperature on the surface quality of amorphous thermoplastic workpieces subjected to single-point turning, and claimed that the glass transition temperature of a polymer, T_g, is the most important, which governs the surface roughness. If the temperature in the cutting zone exceeds T_g, a good surface finish can be achieved and the material would be removed in a ductile manner; otherwise, a rough surface appears because the material would have experienced a process of brittle fracture. Recently, Carr and Feger [14] presented a more detailed analysis of the effect of material properties on the surface roughness of several polymers with different T_g and molecular weights, when subjected to single-point diamond machining. They studied the relationship between the minimum roughness of VESPEL polymer (DuPont, Wilmington, DE) and the tool speed based on the time–temperature superposition principle, [1] and found that the surface roughness would decrease initially when the tool speed increased because of a partial transition into the ductile regime. A further increase in tool speed led to a high deformation rate to which the polymer was unable to respond. As a result, the material ceased to flow and was removed by fracture. For the polymethylmethacrylate (PMMA) polymer, they further concluded that cutting occurred in the melt since they failed to identify any molecular weight effect on the surface roughness.

Clearly, although some efforts have been made to understand the relationship between the surface finish and material properties, there remain many fundamental problems. The increase in cutting speed basically exerts two different stimuli on the mechanical properties of a workpiece material. On one hand, the heat generated will raise the temperature in the cutting zone, increase the long-range mobility of the material's molecular chains, and thus reduce the shear stress and tensile strength. On the other hand, the material will experience a high strain rate, and as a result, will fail at a high tensile strength or shear stress. Hence, the temperature in the cutting zone alone cannot be used as a criterion of the molecular chain mobility at a very high strain rate during machining. In fact, the glass transition temperature, beyond which the movement of molecules becomes possible, tends to increase with the strain rate. Hence, shear stress seems to be a better parameter for characterizing the resultant effect of temperature and strain rate. However, no attempt has been made to clarify the issue when discussing the relationship between the surface roughness and material properties. In addition, the effect of material properties on the shear behavior of polymers, such as the formation characteristics of shear bands during machining, has not been explored, though an understanding of which will offer an insight to the machinability of polymer materials.

---

[1] The time–temperature superposition principle of polymer deformation specifies that the effect of temperature rise on the stress–strain curves of polymers is qualitatively equivalent to that by decreasing the strain rate at deformation.

This work investigates the role of viscous deformation in machining four typical polymer materials that possess different properties. To this end, the study will focus on some key material parameters that influence the quality of surface finish.

2. Material preparation and property measurement

The raw granules of high density polyethylene (HDPE) and low density polyethylene (LDPE) were provided by Qenos Pty Ltd., Australia, and the plates for cutting and property testing were produced by injection moulding. The raw epoxy resin was Araldite-F, a diglycidyl ether of bisphenol A (DGEBA) resin, produced by Ciba-Geigy, Australia. For the preparation of low crosslinked epoxy (LCLE) plates, the following procedures were employed. The epoxy liquid was degassed in a vacuum oven (about $-100 \, \text{kPa}$) at $100°\text{C}$ for about 2 h; then the vacuum was removed and Piperidine hardener was added at a ratio of 100:5 by weight while stirring slowly; the resin was then cast into a preheated mould and cured at $120°\text{C}$ for 16 h. The mould was removed from the oven and allowed to cool gradually to room temperature. To produce highly crosslinked epoxy (HCLE), a different curing agent was used, i.e. $4, 4'$ diaminodiphenyl sulphone (DDS), which has a chemical structure of $C_{12}H_{12}N_2O_2S$ and a molecular weight of 248.31 g/mol, supplied by Merck–Schuchardt, Germany. The Araldite-F resin was mixed with DDS with a weight ratio of 100:32. The curing schedule was as follows: epoxy resin was firstly pre-heated to $135°\text{C}$ in an oven for 30 min; DDS was then added while stirring at the same temperature until it was dissolved completely; the resin was cured for 24 h at $120°\text{C}$ and followed by a 4 h post-cure at $180°\text{C}$; they were then allowed to cool down slowly in the oven in about 10 h.

The effective crosslink density may be assessed by determining the molecular weight between crosslinks M_c. Because the objective of this study is not to determine M_c with high accuracy but to compare epoxy systems with a significant difference in crosslink density, the following empirical relationship between M_c and T_g [15] was adopted:

$$T_g - T_{go} = 3.9 \times 10^4 / M_c, \qquad (1)$$

where T_{go} is the glass transition temperature of the corresponding linear polymer. Bellenger et al. [16] have quoted 364 K as the value of T_{go} for DGEBA/DDS epoxies. $T_{go} = 319$ K for DGEBA/piperidine epoxies was estimated from the empirical relationship between T_{go} and T_g for a number of DGEBA epoxy systems [16].

The M_c values of the piperidine-cured epoxy and DDS-cured epoxy given by the above equation are 810 and 390 g/mol, respectively. Their difference is clearly large. Because the crosslink density is inversely proportional to the molecular weight between crosslinks, the DDS/epoxy system has a larger crosslink density than the piperidine/LR epoxy system. Such a large difference is desirable in the present study as it facilitates the comparison of the effects of crosslink density on the machining behavior of epoxy resins.

The tensile strength (σ_y), elongation at failure (ε_f), glass transition temperature (T_g), melting temperature (T_m) and density (ρ) of these materials were measured and are summarized in Table 1. It can be seen that the thermoplastics, LDPE and HDPE, are very ductile at room temperature because of their low glass transition temperatures and large elongation capacities, while the thermosetting polymers, LCLE and HCLE, are very brittle due to their intrinsic crosslinking characteristics. Based

Table 1
Material properties of the four polymers used in this study

Materials	T_g (°C)	T_m (°C)	σ_y (MPa)	ε_f (%)	ρ (g/cm^3)
LDPE	−109.5	110.6	8	521	0.93
HDPE	−90.4	127.3	18	317	0.95
LCLE	93.4	N/A	68	7.2	1.45
HCLE	192.9	N/A	70	6.5	1.48

on the mobility of the molecular segments, these polymers can be ranked in the order of LDPE, HDPE, LCLE and HLCE.

3. Experiment

Orthogonal cutting was performed at a cutting depth of 0.2 mm using a CNC Minini M286 grinding machine at a series of cutting speeds and a fixed rake angle of $+20°$. In the single-point diamond facing, a diamond cutting edge of radius 8 mm with a fixed rake angle of $+15°$ was used. To keep the feed rate f constant in experiments, the table speed of cutting V in the transverse feed direction was adjusted according to $f = V/\omega$ when the spindle speed ω was varied. The parameter f in a facing operation is similar to the cutting depth in an orthogonal cutting, which controls the thickness of the material removed. The cutting forces in three directions were recorded automatically using a KISTLER 3-component dynamometer (Type 9257B). The surface roughness of a machined surface was measured using a profilometer (Mitutoyo, Surftest 402 Series 178) after an ultrasonic and ethanol cleaning. The cut-off and sampling length in roughness measurements were 0.8 and 4 mm, respectively. Machined surfaces were examined under an optical microscope before and after roughness measurements to identify any possible scratching caused by stylus traveling on the surface. For all specimens in orthogonal cutting, no scratches and surface damage were found. The slight scratches were induced after roughness measurements on very smooth surfaces in the facing operation (HDPE, spindle speed $\omega = 1900$, and feed rate $f = 20, 26$ μm; $\omega = 2500$ rpm and $f = 20, 26$ and 38 μm). Thus in these cases, the real value of surface roughness may be smaller than the measured one. However, this effect is small and does not change the trend of roughness against cutting speed. The morphology of the machined surface was observed using an optical microscope, Leica, and a scanning electron microscope (SEM), Philips 505C, at a voltage of 20 kV.

4. Orthogonal cutting

4.1. Effect of mechanical strength on the surface roughness

Fig. 1 shows the dependence of the surface roughness of HDPE and LDPE specimens on the cutting speed. It shows that the surface finish of both the materials is improved significantly when the cutting speed is increased. However, under the same cutting conditions the HDPE's surface roughness is lower. Considering the fracture stress and mobility of molecular segments of the two
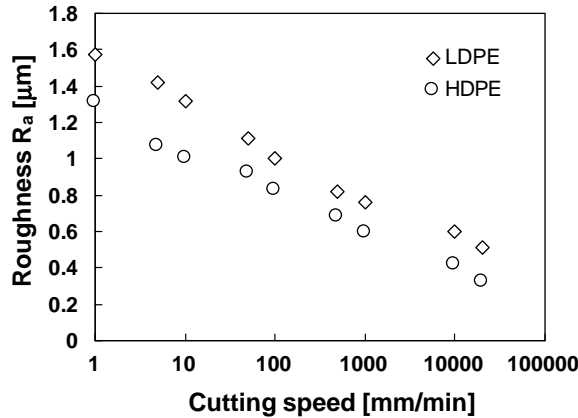
Fig. 1. Surface roughness of LDPE and HDPE versus cutting speed.

materials, the results seem to imply that a too low mechanical strength of a soft polymer prevents a good surface finish. This is understandable if the deformation in the cutting zone is taken into account. In this case, the cutting and thrust forces produce plastic deformation on both the cutting surface and its immediate sub-surface, resulting in a rough machining surface. This is further confirmed in the following discussion about the dependence of shear stress on the cutting speed and the observations of the damaged layer beneath the cutting surface. It should be mentioned that if the T_g of a polymer is far beyond room temperature and the polymer is quite stiff, the surface finish might be improved when a large long-range mobility of molecular segments and a low mechanical strength are achieved [14].

4.2. Shear stress

Fig. 2 depicts the mechanics of an orthogonal cutting process. Fig. 3 shows that the cutting force, F_c, and thrust force, F_t, remain constant after a high peak that signals the first impact contact of the cutting tool with the workpiece. F_c is much larger than F_t.

Due to its viscous behavior, the mechanical properties of a polymer can vary significantly during cutting. Basically, the shear stress of a polymer will increase with strain rate but decrease with temperature. Hence, the shear stress is a good indicator of the resulting influence of both the strain rate and temperature. To see the behavior approximately and qualitatively, let us first use the model for metals [17]:

$$\tau_t = \frac{[(F_c \cos \phi) - (F_t \sin \phi)] \sin \phi}{A_c}, \tag{2}$$

where τ_t is the average shear stress along the chip's shear plane, as illustrated in Fig. 2, A_c is the cross-sectional area of the uncut chip, and ϕ is the shear angle and is given by

$$\tan \phi = \frac{(a_c/a_0) \cos \gamma}{1 - (a_c/a_0) \sin \gamma} \tag{3}$$

where γ is the rake angle of the cutting tool, r_c is the cutting ratio of a_c, the undeformed chip thickness, to a_0, the chip thickness.
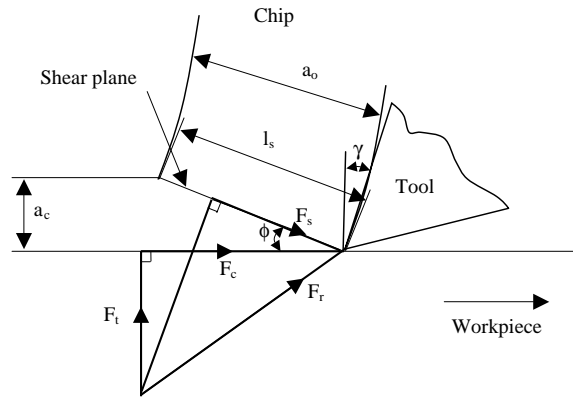
Fig. 2. Mechanics of an orthogonal cutting process, where F_r = resultant tool force, F_c = cutting force, F_t = thrust force, F_s = shear force on the shear plane, ϕ = shear angle, γ = working normal rake, a_c = undeformed chip thickness, a_0 = chip thickness and l_s = length of shear plane.
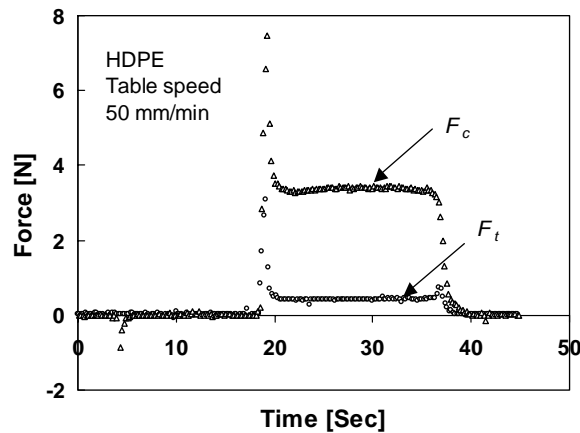

Fig. 3. Recorded cutting force, F_c, and thrust force, F_t, during the machining of HDPE.

As shown in Fig. 4, the shear stresses of both the LDPE and HDPE increase almost linearly with the logarithm of the cutting speed. According to the time–temperature superposition principle, it can be deduced that the increase in strain rate compensated the loss of material strength caused by the temperature rise in the cutting zone. The disturbance applied externally (cutting in this case) is faster than the intrinsic relaxation time of the material at the cutting temperature. Consequently, the material strength increases. Given that the surface roughness of HDPE and LDPE decreases with the cutting speed, the increase in shear stress indicates that a higher mechanical strength results in a better surface finish in cutting very soft polymers that have a great mobility of molecular segments.

It is further noticed that the rate of increase in shear stress of the softer LDPE is faster than that of the harder HDPE, indicating that the effect of the strain rate on the shear stress depends on the material properties. Experimental work on metals [18,19] has shown that the shear stress decreases
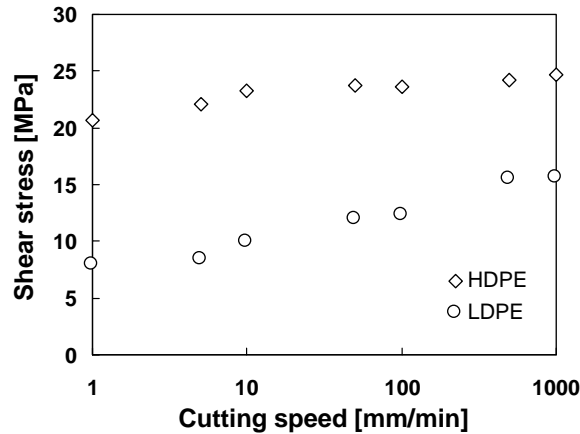
Fig. 4. Calculated shear stress of LDPE and HDPE as a function of the cutting speed.

slightly or remains constant for a given material over a wide range of cutting speeds. Thus, the obvious shear stress increment of the polymers with the strain rate (cutting speed) explored above should be attributed to their intrinsic viscous deformation property. In a polymer, the relationship between stress and strain rate can be described by the Eyring's law [20], i.e., the yield stress σ_y at temperature T increases linearly with the logarithm of the strain rate, $\dot{\varepsilon}$,

$$\sigma_y = \frac{4kT}{\xi V^*}\left(Ln\,\frac{\dot{\varepsilon}}{A} + \frac{\Delta H}{kT}\right),\qquad(4)$$

where ξ is the stress concentration factor, V^* is the activation volume, k is Boltzmann's constant, ΔH is activation enthalpy and A is a constant. Since the strain rate is linearly proportional to the cutting speed [21], Eq. (4) indicates a linear relationship between the shear stress and the logarithm of the cutting speed. This is in good agreement with the experimental result shown in Fig. 4.

4.3. Subsurface damage and surface morphology

A damaged layer beneath the cutting surface was found, whose side view is shown in Fig. 5. The thickness of the layer in the LDPE decreases approximately from 80 μm at the lowest cutting speed of 1 mm/min to 60 μm at the highest speed of 20,000 mm/min. This decrease is ascribed to an increase in strength of the material with the cutting speed, which is consistent with our previous conclusion.

The morphologies of the cut surfaces were examined by an SEM and presented in Figs. 6 and 7 for LDPE and HDPE, respectively, at the two extreme cutting speeds of 1 and 20,000 mm/min. The clear traces of plastic deformation on the cut surfaces were observed in both cases. The low cutting speed brought about severe deformation. Moreover, the cut surface of HDPE is smoother. All these are in good agreement with the surface roughness measurement presented and the discussion above on the material property variation with the cutting speed.
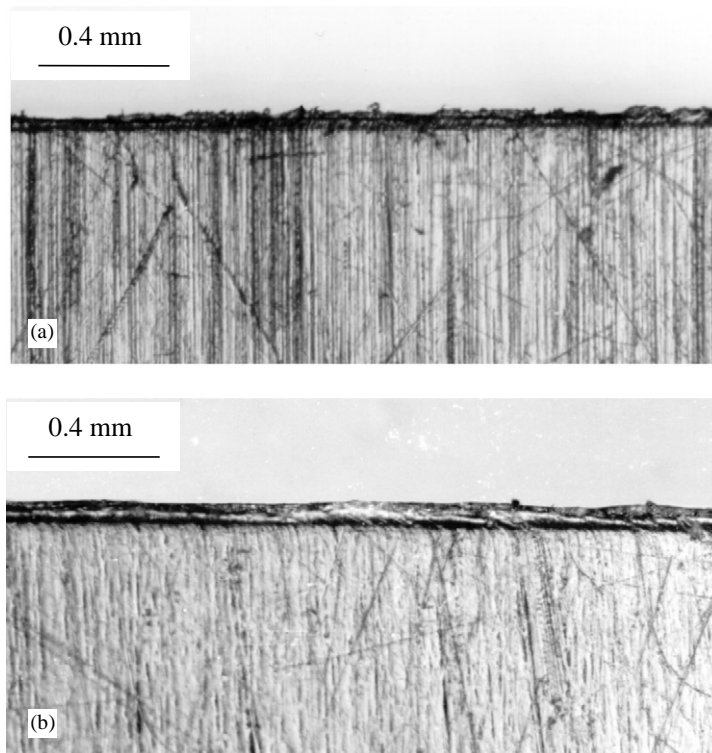
Fig. 5. The damaged layer beneath the cutting surface of LDPE at the cutting speeds of: (a) 1 mm/min; and (b) 20,000 mm/min.
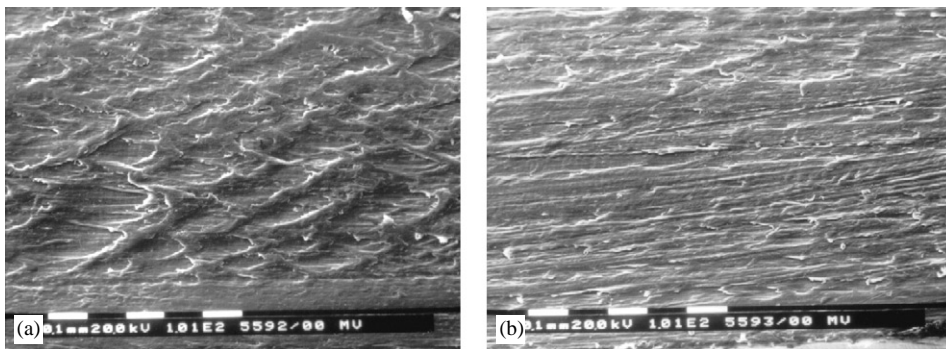

Fig. 6. Machined surface morphology of LDPE at the cutting speeds of: (a) 1 mm/min; and (b) 20,000 mm/min.

4.4. Chip formation

The mechanism of chip formation is of fundamental importance, because it relates the properties of the material to surface integrity, machinability and other machining characteristics. For LDPE and
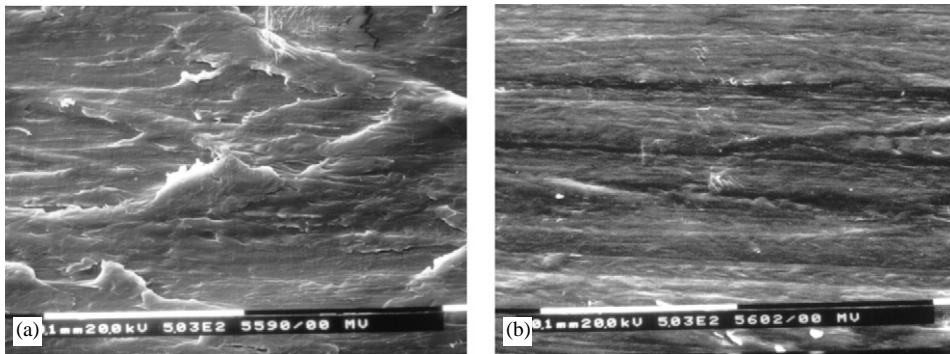
Fig. 7. Machined surface morphology of HDPE at the cutting speeds of: (a) 1 mm/min; and (b) 20,000 mm/min.
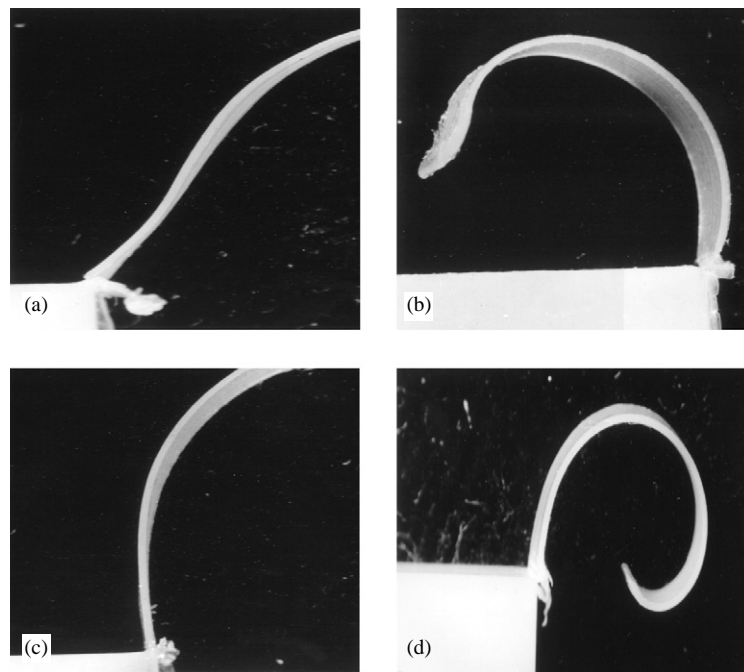

Fig. 8. Continuous curly chips: (a) LDPE at 1 mm/min; (b) LDPE at 20,000 mm/min; (c) HDPE at 1 mm/min, and (d) HDPE at 20,000 mm/min. The cutting tool moved from the right to the left.

HDPE polymers, continuous chips were formed over the entire range of cutting speeds in this study, as shown in Fig. 8. At a low speed, chips curled slightly. With increasing the cutting speed the curling became much severe. By comparing the chip shapes of the two materials, it was found that the LDPE chip curled inwards or clockwise, while the HDPE chips curled and twisted outwards or anticlockwise.

The above phenomenon can be more clearly illustrated using the schematic, Fig. 9, where two different chip formation mechanisms were proposed. It is well known that there are two major
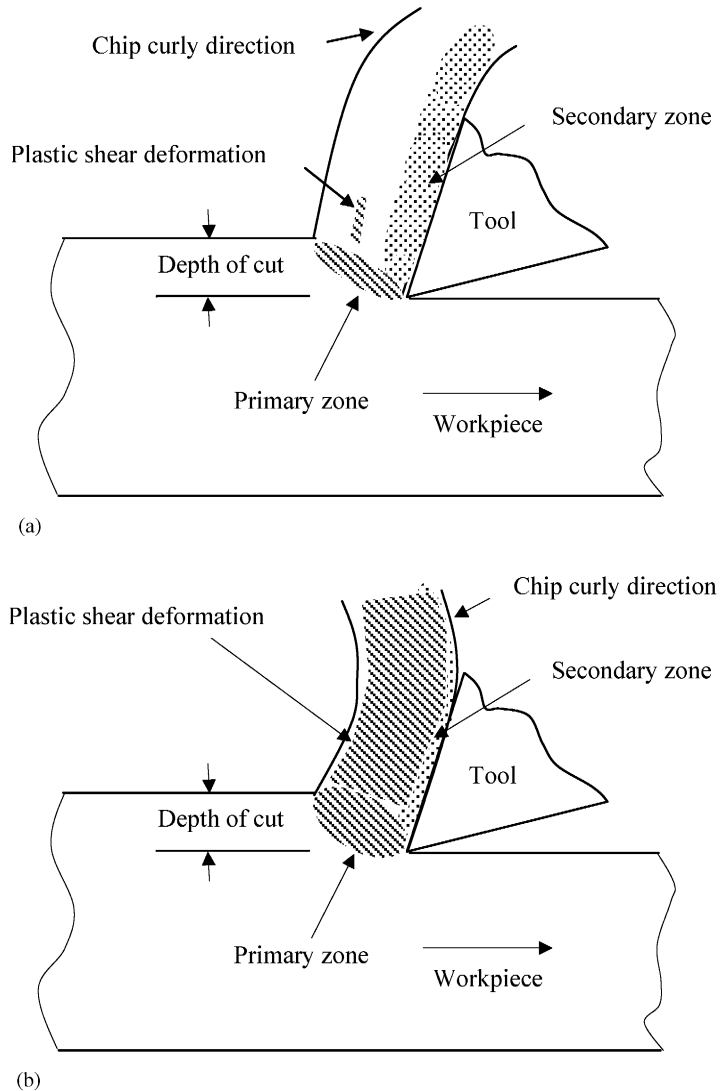
Fig. 9. Chip formation mechanisms in the orthogonal cutting of: (a) an LDPE specimen; and (b) an HDPE specimen.

deformation zones during the chip formation, namely the primary and the secondary zones. Shear deformation occurs in the primary zone to accommodate the deformation caused by the change in material flow direction. When the shear force exceeds the shear yielding strength of the material, plastic shear deformation takes place, leaving a shear deformation band across the chip. Such plastic shear deformation occurs on the shear planes in the direction of the tool movement, thus bends the chip outwards. In the secondary zone, plastic deformation and compressive residual stress twist the chip inwards. As a result, the final twisting direction of the chip is determined by the resultant effect of the above two factors. In relation to the material properties, due to a large elongation of

LDPE before yielding, shear deformation in the primary zone could be elastic with little plastic shear deformation in the chip. However, plastic deformation in the secondary zone in the opposite direction to the chip flow could be significant at a high cutting speed because of the LDPE's low melting point. Consequently, an LDPE chip would curl inwards. On the other hand, an HDPE chip could experience a significant plastic shear deformation but have a smaller and narrower secondary zone, as illustrated in Fig. 9(b), and hence result in a chip bent outwards.

Fig. 10 shows the plastically deformed layers on the chip surfaces and the shear deformation characteristics. In cutting the LDPE, the thickness of the deformation layer in the secondary zone beneath the chip–tool contact surface increases with the cutting speed, which is about 20 µm at 1 mm/min and reaches about 80 µm at 20,000 mm/min. The formation of the layer is ascribed to friction heating at the chip–tool interface. As the frictional heat increases with the cutting speed, the thickness of the layer also increases. The material between the two surface layers in the LDPE chip is not plastically deformed, as shown by the unchanged directions of the fine lines perpendicular to the chip–tool contact surface, marked on purpose before cutting. Thus, the deformation in the middle of a chip is essentially elastic during cutting, which is different from the case in cutting metals. A 'continuous-flow type' chip was reported by Kobayashi [5] and was formed elastically. However, Kobayashi's chip contains no plastic deformation layer near the tool–chip interface and its thickness is equal to the depth of cut. In the present case, however, a clear plastically deformed layer exists. The average chip thickness varies with the cutting speed, from about 235 µm at the cutting speed of 1 mm/min to about 261 µm at 20,000 mm/min when the depth of cut is fixed at 200 µm.

The deformation of a HDPE chip is quite different from that of the LDPE's. In this case, a smoother chip edge and a thinner plastic deformation layer beneath the tool–chip interface were identified (Fig. 10(c)). Further, significant plastic shearing appears in the HDPE chip, indicated clearly by the shear bands across the chip. The difference between the chips of the two materials is attributed to the fact that the LDPE has a lower melting temperature and a greater capacity of sustaining larger shear elastic strain. The melting temperature of LDPE, which is only about 110°C, could have been reached at the tool–chip interface, resulting in a build-up edge. Whilst its greater capacity of large elastic straining prevents plastic deformation in the primary zone. It is interesting to note that the HDPE chip is also different from another type of chip discovered by Kobayashi, the 'continuous-shear chip' [5] that does not have a plastically deformed layer.

4.5. Cutting of epoxies

Two epoxies (LCLE and HLCE) were also cut and the morphology of the cut LCLE surface at the cutting speed of 1 mm/min is shown in Fig. 11. The marks of crack propagations on the very rough surface can be easily identified. The two materials have a close Mode I fracture toughness, about 0.72 MPam$^{1/2}$, and are very brittle. Because of high crosslinking, it is very difficult for these materials to accommodate local deformation through the movement of molecular segments. Hence, they are prone to cracking. Generally, cracks grow more quickly than the movement of the tool edge, which is characterized by a smooth area created by the fast crack propagation (Fig. 11). Since cracks usually propagate in different planes, they bring about a rough surface. On the other hand, the highly concentrated stress in the cutting zone ahead of the tool edge facilitates the crack growth
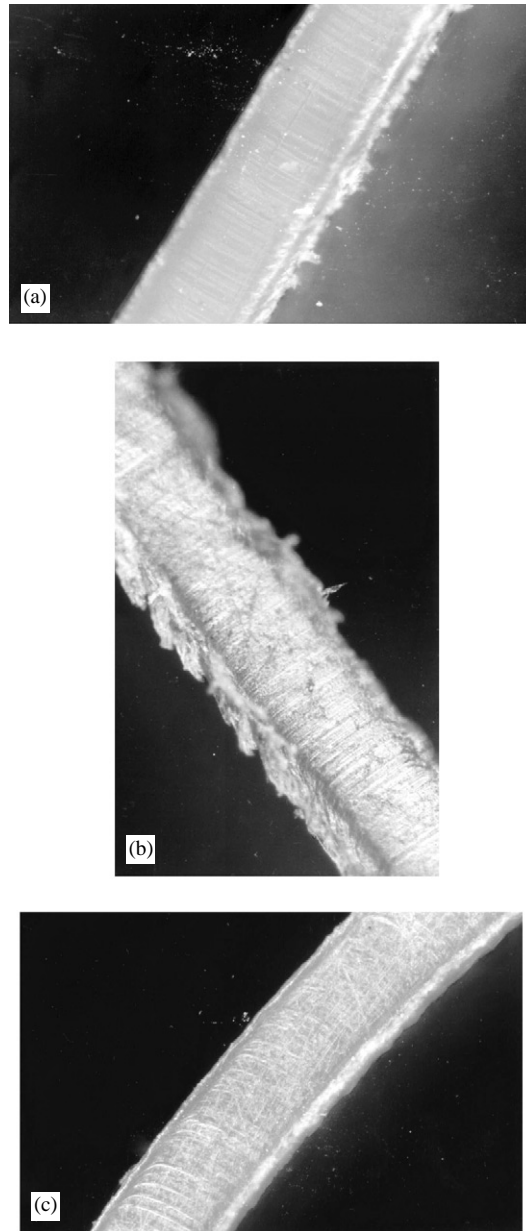
Fig. 10. Build-up edges and shear deformation in chips: (a) LDPE at 1 mm/min; (b) LDPE at 20,000 mm/min; and (c) HDPE at 20,000 mm/min. The surface on the right-hand side is the chip–tool interface. The cutting tool moved from the right to the left.

in a brittle manner, as the initial nucleation sites and the propagation fronts of the cracks showed in Fig. 11. Therefore, orthogonal cutting does not seem to produce smooth surfaces of brittle epoxies under the present machining conditions.
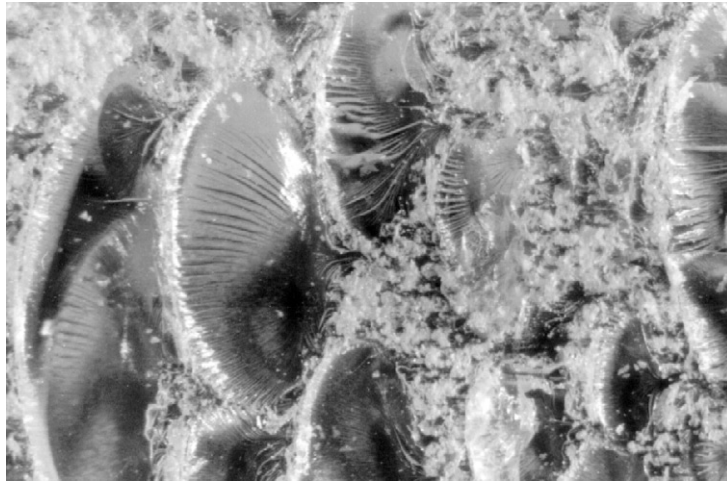
Fig. 11. Machined surface morphology of LCLE at the cutting speed of 1 mm/min.

5. Facing

5.1. Thermoplastics

5.1.1. LDPE—mechanism of surface integrity

The surface roughness of the machined LDPE as a function of the spindle speed ω is depicted in Fig. 12. Three sets of experiments were conducted in order to separate the effect of feed rate f. In the first group, the feed rate *was* changed from 500, 71, 38, 26 to 20 μm with the increasing ω from 100 to 2500 rpm (solid line with circles). An optimal spindle speed of 1300 rpm was obtained to minimize the surface roughness. In the second set, f was kept constant at 38 μm (dashed line with triangles). Similarly, the best surface quality was obtained at the spindle speed of 1300 rpm. In the last set, ω was fixed at 1300 rpm while f was decreased from 500, 71, 38, 26 to 20 μm (from top square to the bottom in Fig. 12). It is seen that the surface roughness gradually decreases with decreasing feed rate. The increase in surface roughness beyond the spindle speed of 1300 rpm was a result of the spindle speed effect rather than that of the feed rate. An inspection of the machined surfaces revealed that the specimens cut beyond 1300 rpm contain extensive surface scales whose size reaches about 2 mm in length when ω increases to 2500 rpm, which makes the surface much rougher.

The surface morphologies of LDPE at the feed rate of 38 μm and different spindle speed were observed under SEM and presented in Fig. 13. At a low spindle speed of 100 rpm, the scales as large as 50 μm can be identified and they appeared evenly on the surface. Both the size and number of the scales decreased as ω increased and reached their minima at 1300 rpm. However, when the spindle speed increased further, they increased. The microphotos in Fig. 13 show clearly that the scales are induced by stretched flows of the surface material and scaling happens in the direction of the cutting speed. Therefore, it is reasonable to conclude that the cutting temperature beyond 1300 rpm became much higher, which made the mechanical strength of the material much lower and introduced localized visco-plastic deformation. Melting of the material might have occurred in
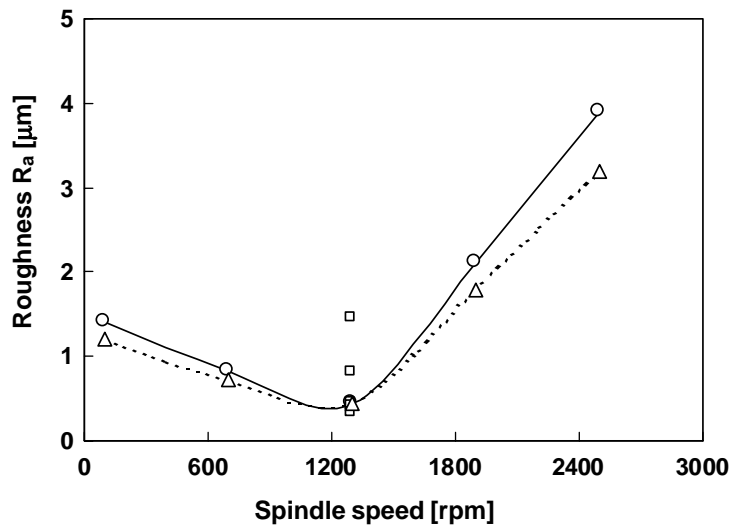
Fig. 12. Surface roughness of the machined LDPE as a function of the spindle speed: ($\triangle$) feed rate f remained unchanged at 38 μm; ($\circ$) f changed from 500, 71, 38, 26 to 20 μm as the spindle speed increases from 100 to 2500 rpm; ($\square$) f changed from 500, 71, 38, 26 to 20 μm (top to the bottom).

the top thin layer of the machining surface. Since LDPE has a low glass transition temperature and mechanical strength (Table 1), the scaling is prone to happening. The above roughness measurement and morphology observation on scaling indicate that the improvement of the surface roughness with increasing the spindle speed in the range from 100 to 1300 rpm is associated with the "hardening" of the material, where the effect of strain rate dominates. This is similar to that observed in orthogonal cutting. When the cutting temperature becomes a dominant factor (spindle speed > 1300 rpm), the viscous deformation of the polymer starts to play a more important role in the material removal and more intensive scaling via viscous-flow takes place. Hence, an effective way to eliminate the scaling and thus to improve the surface finish at a high spindle speed is to apply sufficient coolant in cutting.

5.1.2. HDPE—surface roughness and strain-rate hardening

The effect of spindle speed on the surface roughness of thermoplastic HDPE at different feed rates is displayed in Fig. 14. As expected, the roughness of the machined surface decreases with decreasing f. This is because the thickness of the layer removed in each revolution decreases. At a large feed rate, e.g. 500 μm, the surface roughness remains almost unchanged with increasing the spindle speed, because the roughness in this case is determined by the cutting marks (Fig. 15(a) and (b)). When the feed rate decreases to 71 μm, a smoother surface can be seen under the optical microscope (Fig. 15(c)). At a small feed rate, however, the effect of ω becomes significant and the surface quality is improved as the speed increases. An inspection of the machined surfaces ($f = 20$ μm) showed that a surface cut at $\omega = 2500$ rpm is very bright while that at $\omega = 100$ rpm appears diffusive. The SEM images in Fig. 16 show that the cutting marks become much thinner and the surface area becomes smoother when the spindle speed increases from 100 to 2500 rpm with a constant feed rate.
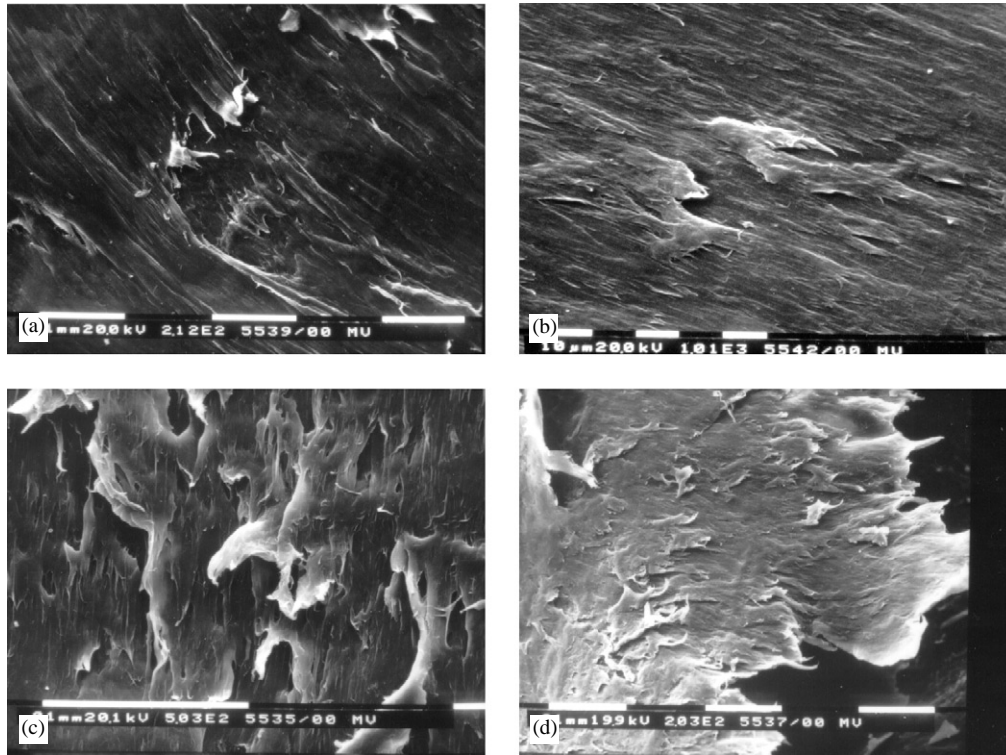
Fig. 13. Surface morphologies of LDPE at different facing conditions ($f = 38$ μm): (a) $\omega = 100$ rpm; (b) $\omega = 1300$ rpm; and (c) and (d) $\omega = 2500$ rpm.

A comparison of surface finish reveals that the surface roughness of HDPE is better than that of LDPE under the same cutting conditions. For example, the former is 0.26 μm and the latter is 0.44 μm when $\omega = 1300$ rpm and $f = 0.38$ μm. This is consistent with the result of orthogonal cutting and again confirms that a high mechanical strength is preferred in order to produce a good surface finish. Moreover, the comparison seems to indicate that the surface roughness improvement of HDPE under a higher spindle speed is attributed to the hardening of the material induced by a higher strain rate. The absence of scaling in the HDPE specimens can be attributed to its relatively high glass transition temperature and mechanical strength.

5.2. Epoxies

5.2.1. Surface roughness

Highly and low crosslinked epoxies (HCLE and LCLE) were cut to evaluate the effect of molecular mobility in very brittle thermosetting materials on their machinability during facing operation. The variation of their surface roughness with the spindle speed is shown in Fig. 17. The effect of the feed rate on the roughness appears only at low spindle speeds. It seems that the surface roughness of both the HCLE and LCLE is independent of the spindle speed when f is constant.
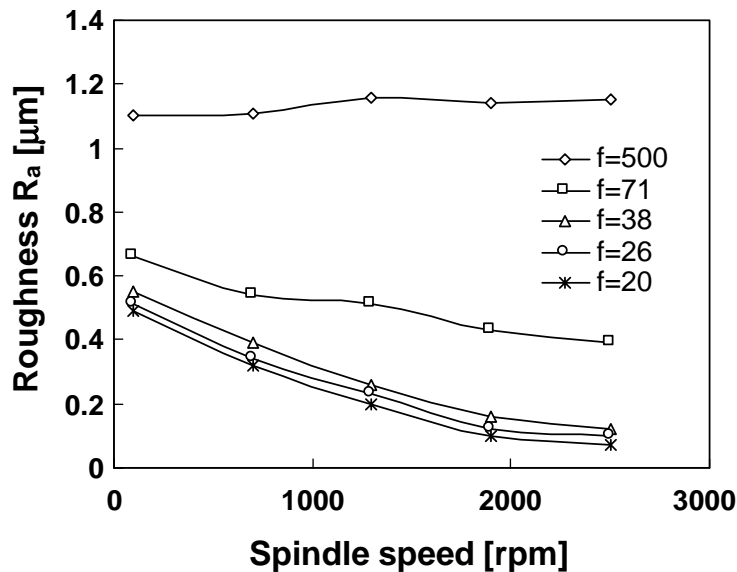
Fig. 14. Surface roughness of the machined HDPE as a function of the spindle speed. The unit of the feed rate f is micrometre.

However, it is worth noting that the roughness of the HCLE is always lower than that of the LCLE.

5.2.2. Cutting in the rubbery plateau region

As is well known, the variation of mechanical properties of a crosslinked epoxy with increasing temperature is quite different from that of linear polymers. Above T_g, a crosslinked epoxy will enter its rubbery plateau region and become a rubber-like material where the elasticity is characterized by a high elongation at break and a low modulus. The molecular chains of a crosslinked epoxy in this region are hindered from moving past each other over a long distance. Considering that T_g of the LCLE is almost 100°C lower than that of the HCLE (192.9°C), it is highly likely that the cutting of the LCLE occurred in the rubbery plateau region. The chips were very small, much like dust particles. Consequently, a rough surface was formed. This is consistent with the observation of Car and Feger [14], who machined a vulcanized polybutadiene rubber.

5.2.3. Surface morphology

The SEM surface images of the machined HCLE and LCLE under different cutting conditions are displayed in Fig. 18. At a large feed rate and a low spindle speed, the machined surfaces of the two materials are very similar and are of the nature of brittle fracture. The areas created by crack propagation are evident. The initial fronts of crack propagation due to stress concentration can also be seen. These fronts demonstrate that the materials are hard and a great stress is needed to drive a crack to grow. At a small feed rate and a large spindle speed, however, the cut surfaces of the two materials become different. Large crack propagation marks are rare on the HLCE surfaces but cracking can be still identified. The material seems quite brittle and still has a relatively high
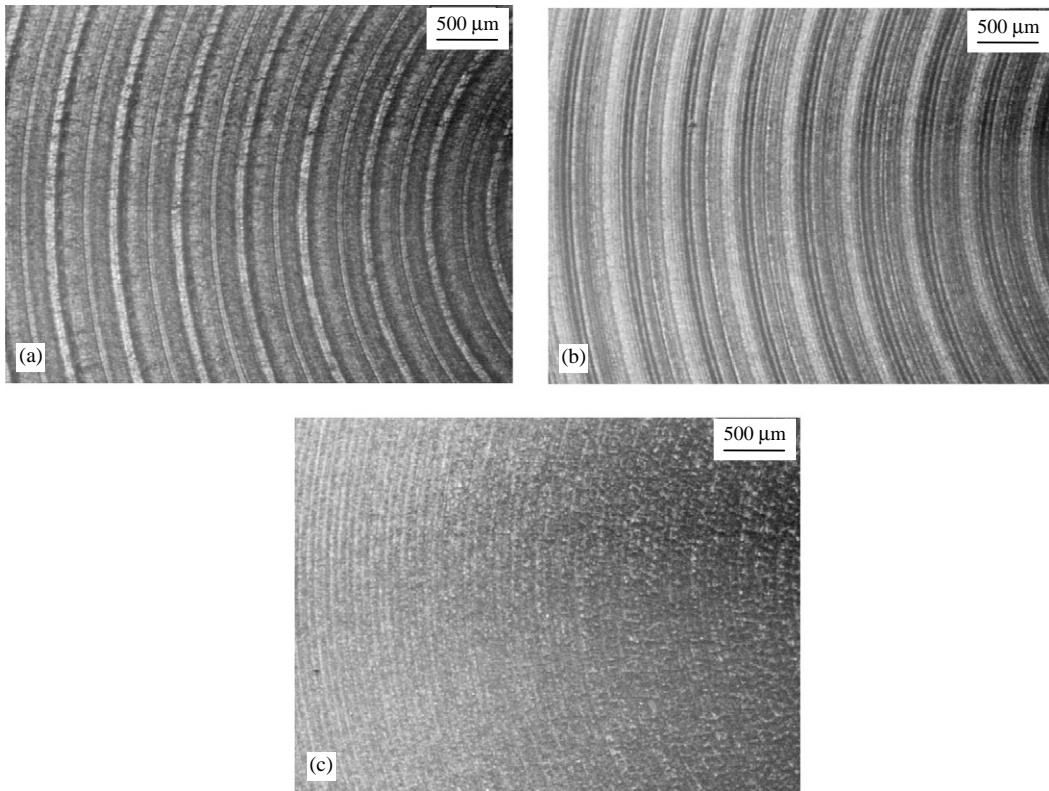
Fig. 15. Surface morphologies of HDPE at different facing conditions: (a) $\omega = 100$ rpm, $f = 500$ μm; (b) $\omega = 2500$ rpm, $f = 500$ μm; and (c) $\omega = 2500$ rpm, $f = 71$ μm.
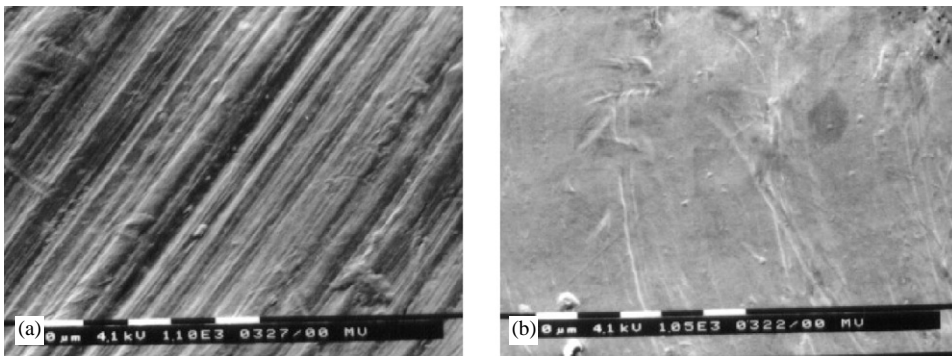

Fig. 16. Surface morphologies of HDPE at different facing conditions: (a) $\omega = 100$ rpm, $f = 38$ μm; and (b) $\omega = 2500$ rpm, $f = 38$ μm.

modulus. The LCLE surfaces possess many small flat areas that have very much the features of tearing. No crack fronts and cracking can be identified in this case and the modulus of the material seems very low. Such surface characteristics strongly suggest that the temperature during machining
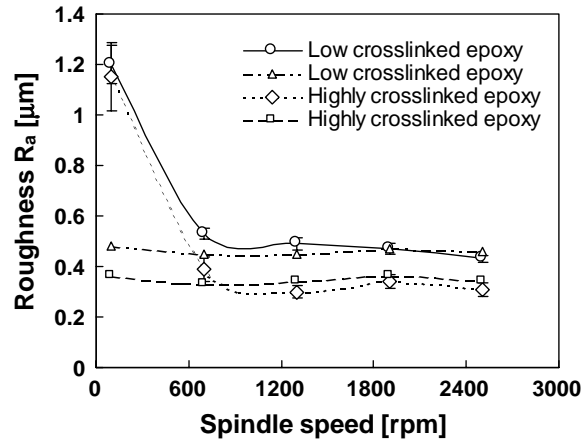
Fig. 17. Surface roughness of the machined HCLE and LCLE as a function of the spindle speed: ($\triangle$) and ($\square$), feed rate f remained unchanged at 20 μm; ($\circ$) and ($\diamond$), f changed from 500, 71, 38, 26 to 20 μm as the spindle speed increases from 100 to 2500 rpm.

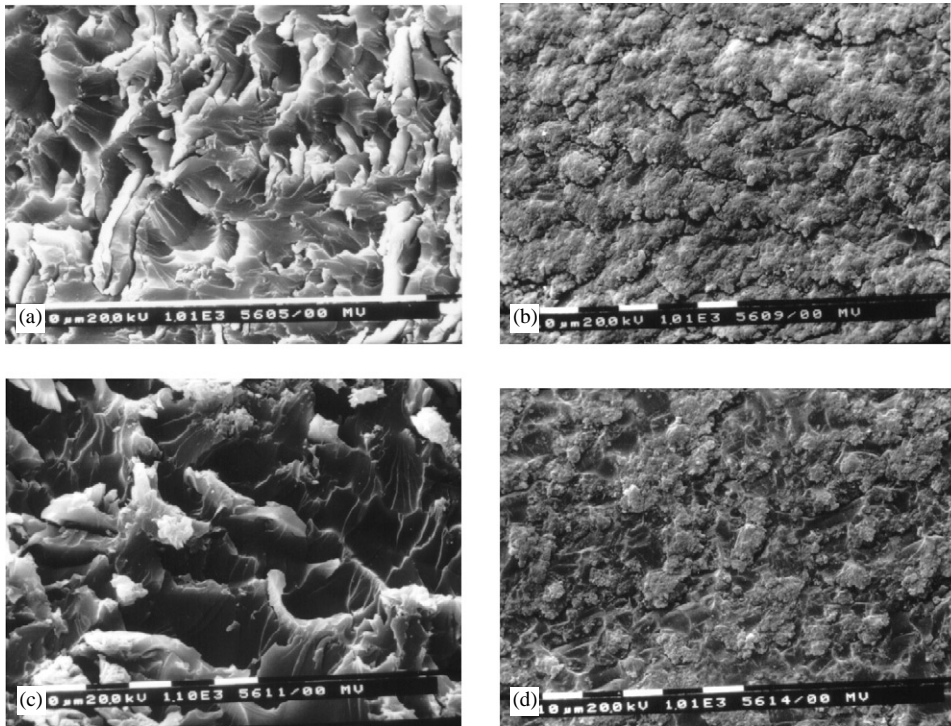

Fig. 18. Surface morphologies of epoxies: (a) HCLE, $\omega = 100$ rpm, $f = 500$ μm; (b) HCLE, $\omega = 2500$ rpm, $f = 20$ μm; (c) LCLE, $\omega = 100$ rpm, $f = 500$ μm; and (d) LCLE, $\omega = 2500$ rpm, $f = 20$ μm.

LCLE be larger than its T_g and the material removal occur in the rubbery plateau region. Thus, a smooth surface of a polymer is difficult to obtain due to its high brittleness below T_g but rubber-like behavior above T_g. The chips of both HCLE and LCLE are powder-like. However, the size of the latter is much larger, which is in good agreement with the surface morphology shown in Fig. 18.

6. Conclusions

In this study, orthogonal cutting and facing by a single point diamond were performed on four typical polymers. Two of them (LDPE and HDPE) are thermoplastics with very low glass transition and melting temperatures, and the other two are crosslinked thermosetting polymers (LCLE and HCLE), which are very brittle. The mechanisms of surface integrity and machinability were discussed in relation to the variation of material properties and machining conditions. The following conclusions can be drawn:

(1) The viscous properties of a polymer play a decisive role in determining the machined surface quality. Because the viscous deformation depends strongly on the strain rate and temperature, a proper selection of machining parameters is very important and can minimize the surface roughness. To avoid excessive viscous–plastic scaling/tearing at a high speed cutting, for example, sufficient coolant needs to be applied.

(2) The shear stress in orthogonal cutting is a good measure for evaluating the coupled effect of strain rate and temperature in the cutting zone. A relatively large shear stress corresponds to a smoother machining surface of a very soft polymer that has low T_g (or T_m) and mechanical strength.

(3) The surface roughness of the thermoplastic with higher glass transition temperature and mechanical strength is generally smaller. The surface finish of thermoplastics can be improved by increasing the cutting speed. However, the effect of temperature rise at high speed of cutting can be more significant than that of the strain rate.

(4) Two new types of chips were discovered in the orthogonal cutting of the thermoplastics. The deformation in the primary and the secondary zones strongly depend on the material properties, particularly on the yielding strain of shear and T_g (or T_m). A large yielding strain could restrain shear deformation in the primary zone within the elastic regime of the material, while a low T_m could lead to a larger secondary zone.

(5) It is difficult to obtain a smooth surface of crosslinked thermosetting polymers since the materials are unable to deform plastically or flow over a long distances. The material removal is via cracking when the local cutting temperature is below T_g. If it is above T_g, the material will become rubber-like and the material removal is via tearing.

References

[1] Donaldson RR, Patterson SR. Design and construction of a large, vertical axis diamond turning machine. Proceedings of the SPIE 1983;433:62–7.

[2] DeBra DB. Design of laminar flow restrictors for damping pneumatic vibration isolators. CIRP Annals 1984;33:351–61.

[3] Donaldson RR, Maddux AS. Design of a high-performance slide and drive system for a small precision machining research lathe. CIRP Annals 1984;33:243–8.

[4] Franse J. Manufacturing techniques for complex shapes with submicron accuracy. Reports on Progress in Physics 1990;53:1049–94.

[5] Kobayashi AK. Machining of plastics. New York: McGraw-Hill, 1967.

[6] Decker DL, Grandjean DJ. Physical and optical properties of surface generated by diamond-turning on an advanced machine. NBS Special Publication 1978;541:122–31.

[7] Kobayashi AK. Ultra-precision machining of plastics. SPIE 1984;508:34–6.

[8] Kobayashi AK. Machining of plastics: Part I. Modern Plastics 1963;43:110.

[9] Kobayashi AK. Machining of plastics: Part II. Modern plastics 1963;43:109.

[10] Young AE, Wilson JH. The critical rake angle in the machining of plastics. Plastics and Rubber: Processing 1978;3(9):77–84.

[11] Jiang Q, Zhang LC, Pittolo M. The dependence of surface finish of a spectacle polymer upon machining conditions. In: D. Chen et al., editors. Progress of Machining Technology. Beijing: Aviation Industry Press, 2000. p. 7–12.

[12] Kobayashi AK, Saito K. On the cutting mechanism of high polymers. Journal of Polymer Science 1962;58:1377–95.

[13] Smith EF. Single-point turning of amorphous thermoplastic polymers. MS thesis, North Carolina State University, Raleigh, NC, 1989.

[14] Carr JW, Feger C. Ultraprecision machining of polymers. Precision Engineering 1993;15:221–37.

[15] Kishi H, Shi YB, Huang J, Yee AF. Shear ductility and toughenability study of highly cross-linked epoxy/polyethersulphone. Journal of Material Sciences 1997;32:761.

[16] Bellenger V, Verdu J, Morel E. Effect of structure on glass transition temperature of amine crosslinked epoxies. Journal of Polymer Science. Part B 1987;25:1219.

[17] Boothroyd G. Fundamentals of metal machining and machine tools. New York: McGraw-Hill, 1975. p. 74.

[18] Chao BT, Bisacre GH. The effect of speed and feed on the mechanics of metal cutting. Proceeding of the Institution of Mechanical Engineers 1951;165:1–13.

[19] Wallace PW. An investigation on the friction between chip and tool in metal cutting. Fellowship thesis, Department of Mechanical Engineering, University of Salford, England, 1962.

[20] Bucknall CB. Toughened plastics. London: Applied Science, 1977.

[21] Lei S, Shin YC, Incropera FP. Material constitutive modeling under high strain rates and temperatures through orthogonal machining tests. Journal of Manufacturing Science and Engineering 1999;121:577–85.